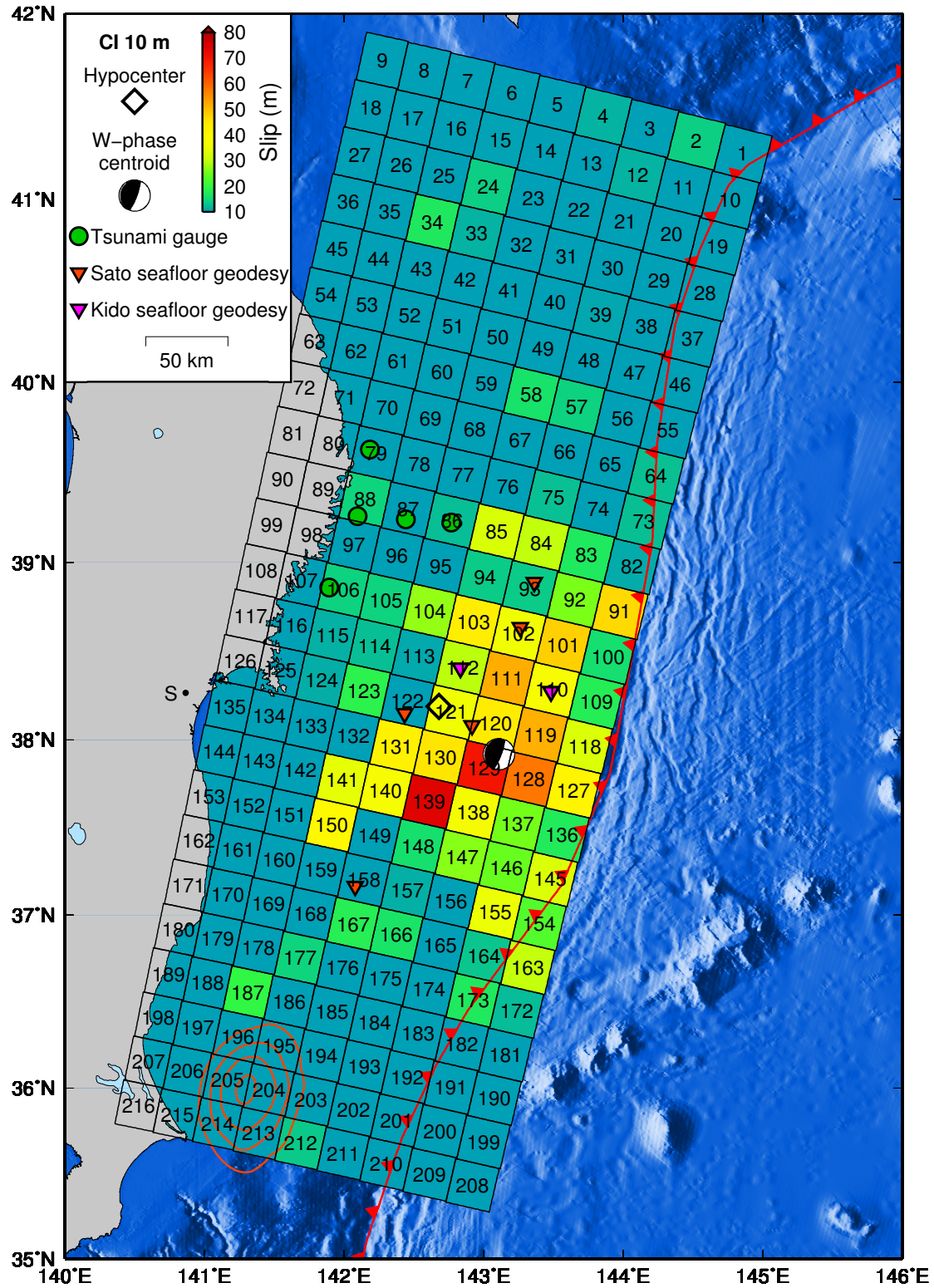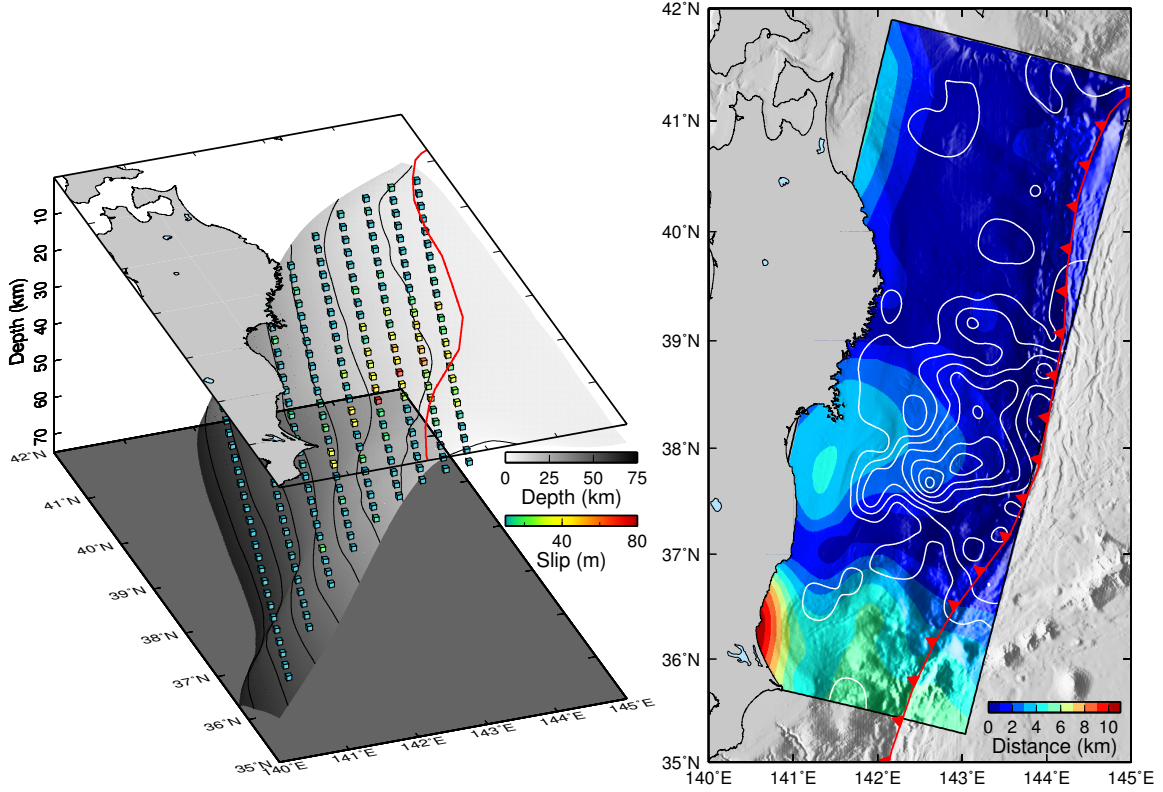# Supplementary material for "Bayesian inversion for finite fault earthquake source models II — The 2011 great Tohoku-oki, Japan earthquake"

S. E. Minson, M. Simons, J. L. Beck, F. Ortega, J. Jiang,
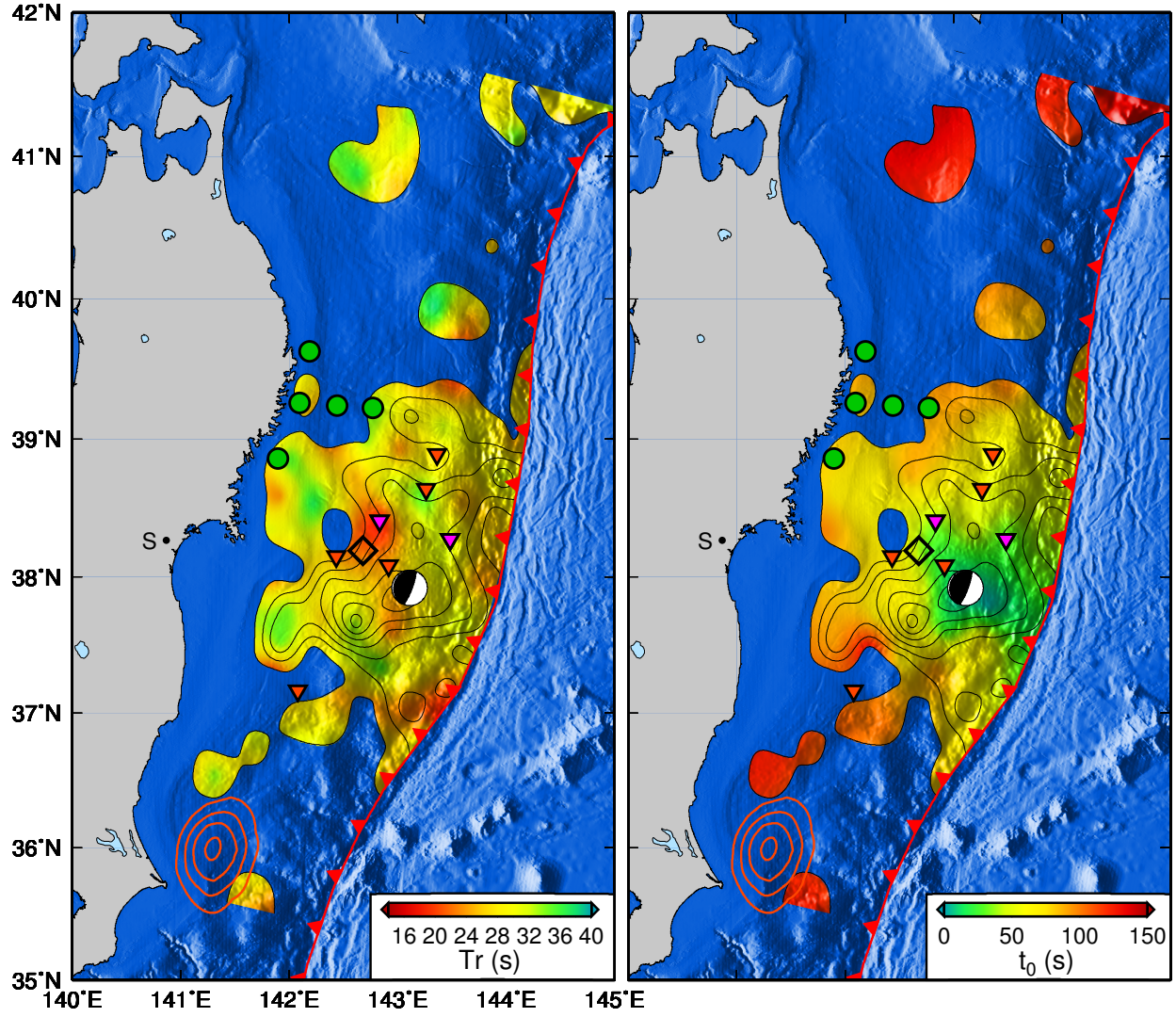S. E. Owen, A. W. Moore, A. Inbal, and A. Sladen

May 4, 2014

Supplementary Figure 1: Key to fault patches. The mean posterior slip model from the joint static-kinematic inversion is shown. Detailed information about each fault patch is given in Table S1.
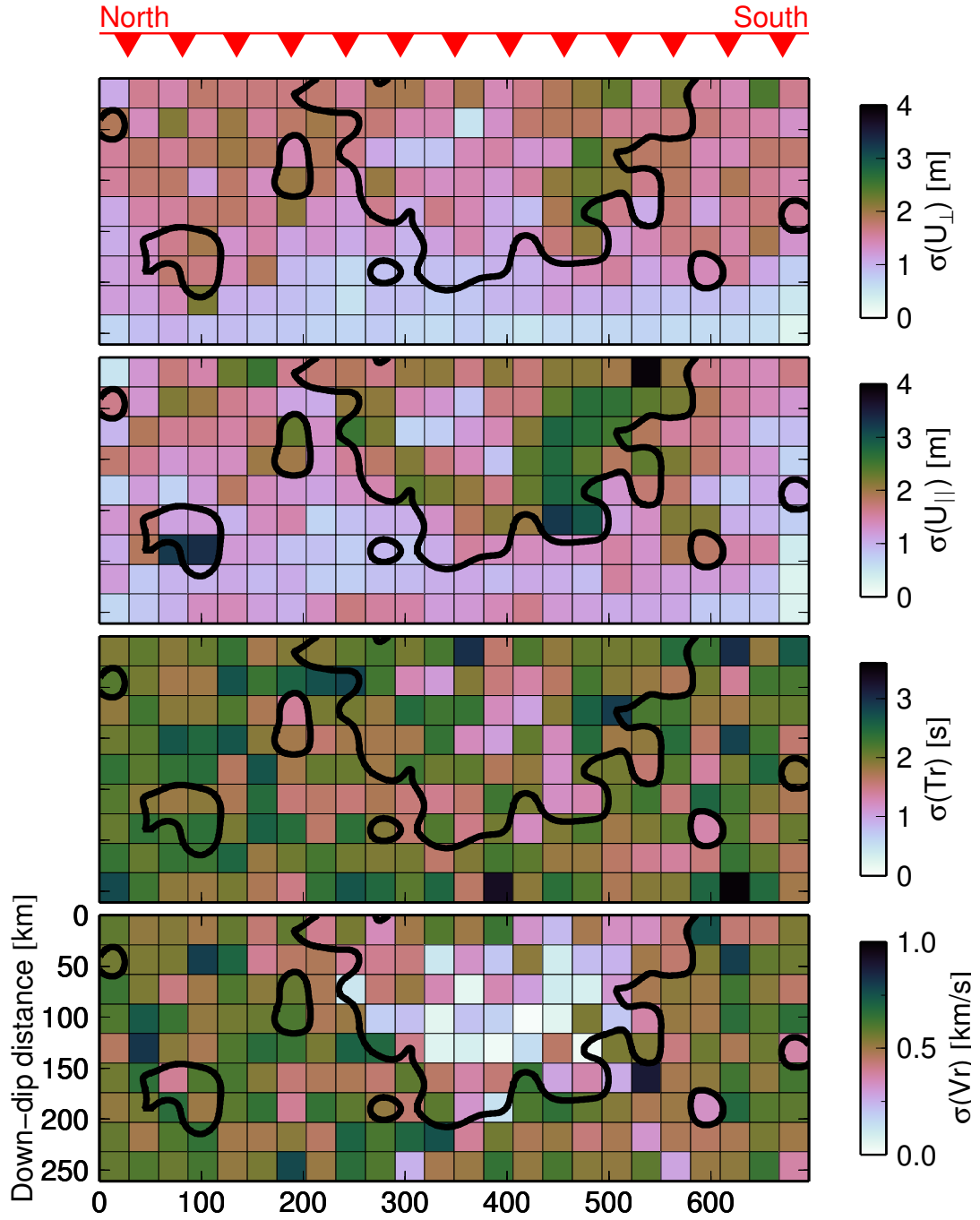
Supplementary Figure 2: (Left) Comparison between regularly gridded fault geometry used in inversions (cubes) with 3-D Japan trench slab geometry. (Right) Distance between regularly gridded fault and the surface of the megathrust. Contours of the mean posterior kinematic slip model (Fig. 2) are plotted using a contour interval of 10 m. Note that the distance between the regularly gridded fault and the megathrust are less than a few kilometers in all regions of significant slip.
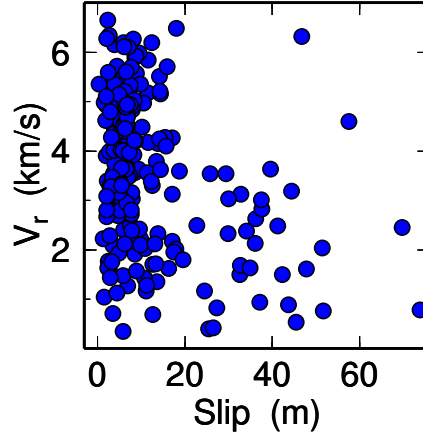
Supplementary Figure 3: Mean of posterior slip duration (left) and time of rupture initiation (right) from joint kinematic-static inversion. All symbols are the same as in Fig. 2. Mean posterior slip model is plotted with black contour lines in increments of 10 m.
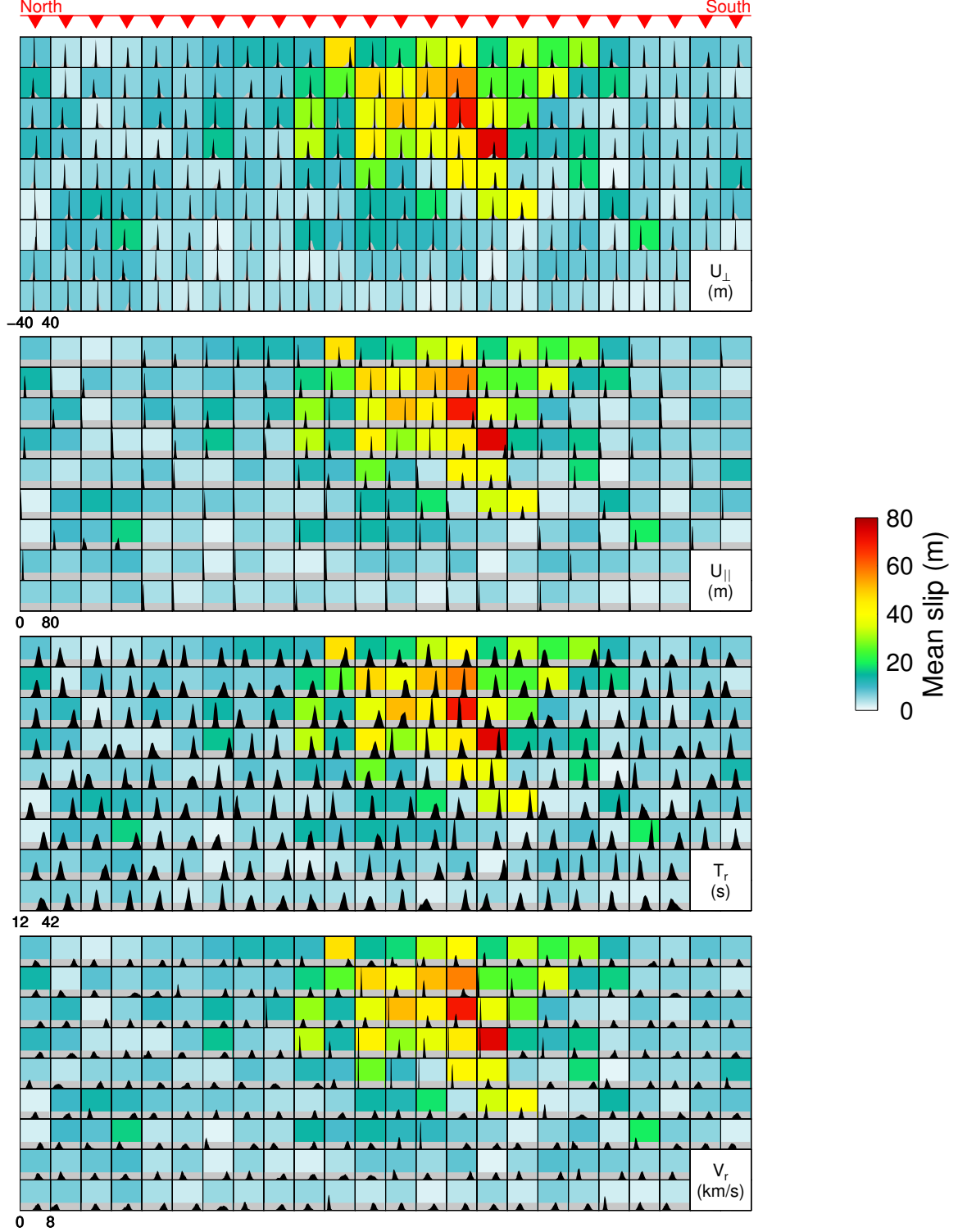
Supplementary Figure 4: Standard deviations of the posterior PDF for each rupture parameter for the kinematic inversion. The fault is oriented so the the trench is aligned with the top edge of the fault plane, north is on the left side of this figure, and south is on the right side. The 10 m contour line from the mean of the posterior slip distribution is plotted for reference. Rupture velocity is significantly better constrained inside the region of largest slip.

Supplementary Figure 5: Rupture velocity versus slip amplitude of the posterior mean kinematic rupture model.

Supplementary Figure 6: Prior and posterior PDFs from the kinematic inversion. The fault is orientated so that the trench parallels the top edge of the plot, north is to the left, and south is to the right. The gray PDFs are the prior distribution, while the posterior PDFs are shown in black. (The prior PDF on $U_\perp$ is exact while the uniform prior PDFs have been vertically scaled to increase visibility.) The background color of each patch is the mean posterior slip. From top to bottom are shown strike-slip motion, dip-slip motion, slip duration, and rupture velocity.

7

List of Supplementary Tables

The following tables are provided as separate text files.

Table S1 Fault geometry

Table S2 GPS static offsets

Table S3 GPS-acoustic seafloor displacements from Kido et al. (2011)

Table S4 GPS-acoustic seafloor displacements from Sato et al. (2011)

Table S5 Near-coast tsunami instruments

Table S6 DART deep water tsunami instruments

Table S7 1 Hz kinematic GPS station locations

Description of Additional Supplementary Files

A set of text files are provided that describe the posterior PDF from the kinematic inversion. Each file has 866 lines corresponding to the 866 free parameters in the inversion. The first 216 lines describe the strike-slip (rake=0°) component of motion, in meters, on each of the 216 fault patches in the order they are listed in Table S1. The second 216 lines describe the dip-slip (rake=90°) component of motion in meters. The third 216 lines describe the duration of the source-time-function for each patch in seconds. The fourth 216 lines describe the rupture velocity for each patch in km/s. The final two lines describe the location of the hypocenter in kilometers along-strike and kilometers down-dip, respectively.

posterior_mean.txt Sample mean of the posterior PDF: $\bar{\theta} = \frac{1}{N} \sum_{i=1}^{N} \theta_i$.

central_moment2.txt Second central moment of the posterior PDF: $\frac{1}{N} \sum_{i=1}^{N} (\theta_i - \bar{\theta})^2$.

central_moment3.txt Third central moment of the posterior PDF: $\frac{1}{N} \sum_{i=1}^{N} (\theta_i - \bar{\theta})^3$.

central_moment4.txt Fourth central moment of the posterior PDF: $\frac{1}{N} \sum_{i=1}^{N} (\theta_i - \bar{\theta})^4$.

posterior_correlation.txt Posterior correlation matrix.